Visualization and void fraction measurement of gas-liquid two-phase flow in a commercial plate heat exchanger by thermal neutron radiography

Asano, Hitoshi
Takenaka, Nobuyuki
Fujii, Terushige
Hayashi, Hidenori
Wakabayashi, Toshiaki

(Citation)
IEEE transactions on nuclear science,52(1):280-284

(Issue Date)
2005-02

(Resource Type)
journal article

(Version)
Version of Record

(URL)
https://hdl.handle.net/20.500.14094/90000215

Visualization and Void Fraction Measurement of Gas-Liquid Two-Phase Flow in a Commercial Plate Heat Exchanger by Thermal Neutron Radiography

H. Asano, N. Takenaka, T. Fujii, H. Hayashi, and T. Wakabayashi

***Abstract*—Adiabatic air–water two-phase flows in a commercial plate heat exchanger were visualized by thermal neutron radiography method as a nondestructive test in order to clarify liquid distributions. Liquid distributions in a single channel and a multichannel plate heat exchanger were investigated. From the results of a single channel, it was shown that gas phase tended to flow at the center of the net-like conduit and liquid fraction at the both side was higher. However, in the case of higher gas volumetric flux above 19 m/s, liquid distributions seemed to be homogenous. Measured average void fractions were lower than those by the homogenous model. On the other hand, from the results of a multichannel, it was shown that liquid distribution into the each channel strongly depended on inlet conditions. In the case of higher liquid flow rate and lower gas flow rate, liquid fraction became higher with the deeper channel due to larger liquid momentum. However, in the case of lower liquid flow rate and higher gas flow rate, the opposite tendency of liquid distribution was observed, that is to say, liquid fraction was lower with the deeper channel.**

***Index Terms*—Flow distribution, gas-liquid two-phase flow, neutron radiography, plate heat exchanger, void fraction.**

I. Introduction

THE plate heat exchanger is widely used in industrial process, such as chemical process, food processing, oil cooling systems, and so on. In most cases, it is used as a liquid heat exchanger. Recently, applications of plate heat exchangers to gas-liquid two-phase flows have become of interest for their compactness and the heat transfer performance improvement. A schematic configuration of a commercial plate heat exchanger is shown in Fig. 1. A plate heat exchanger is made by brazing 20 to 280 sheets of stainless steel wavy plates. Working fluids flows through the gaps between these plates. The channel of each fluid is arrayed alternately, that is, a plate heat exchanger has many parallel channels. In the case where working fluids flow in a plate heat exchanger as gas-liquid two-phase mixtures, the dynamic behaviors of gas-liquid two-phase flow greatly affect the heat transfer performance. In order to design or improve heat exchange for gas-liquid two-phase flows, such as evaporators and condensers, it is important to understand the liquid distribution not only into parallel channels, but also in the each channel. In particular, in the case where the inlet flow is a two-phase flow, the effect of inlet flow conditions on the liquid distribution is should be clarified.

Manuscript received September 20, 2002; revised August 31, 2004.

The authors are with the Department of Mechanical Engineering, Kobe University, Kobe, Hyogo 657-8501, Japan (e-mail: asano@mech.kobe-u.ac.jp; takenaka@mech.kobe-u.ac.jp; fujii@mech.kobe-u.ac.jp).

Digital Object Identifier 10.1109/TNS.2005.843676

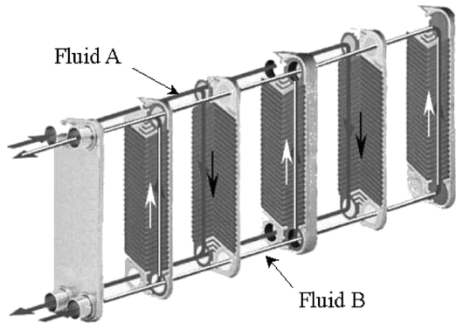

Fig. 1. Plate heat exchanger.

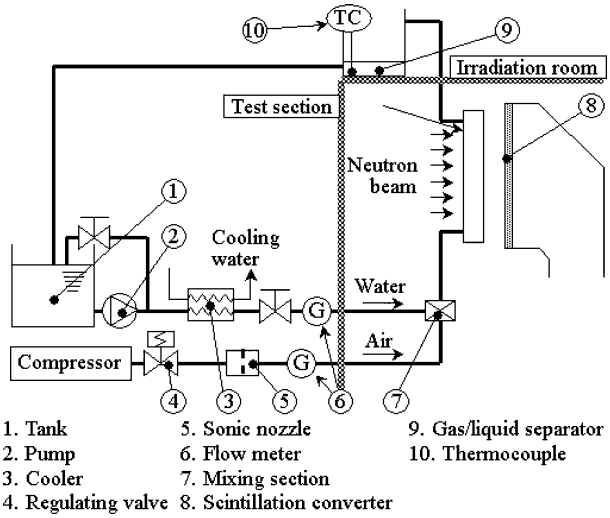

Fig. 2. Schematic diagram of experimental apparatus.

There are many papers on flow and heat transfer characteristics of liquid single-phase flows in plate heat exchangers, and the performance prediction method with the consideration of geometric parameters has been proposed in [1]. However, there are few papers on gas-liquid two-phase flow characteristics only in a single channel [2]–[4], and there are no papers on a plate heat exchanger with parallel channels. The authors also visualized adiabatic and boiling two-phase flows in a simulated single-channel plate heat exchanger by neutron radiography and considered liquid distributions [5].

In this paper, to understand the existing condition and problem in gas-liquid two-phase flow application, adiabatic air-water two-phase flows in a commercial plate heat exchanger with single and multichannels were visualized as a nondestructive test on flow structures by neutron radiography.

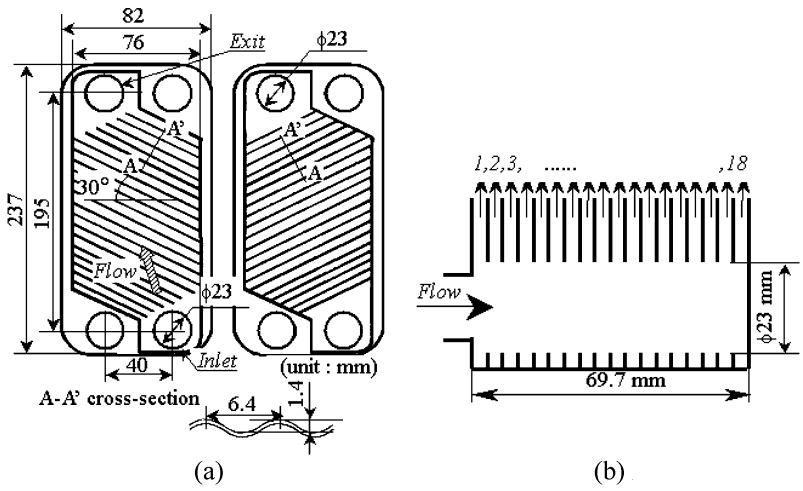

Fig. 3. Configuration of plate heat exchanger. (a) Plate and (b) distributing header.

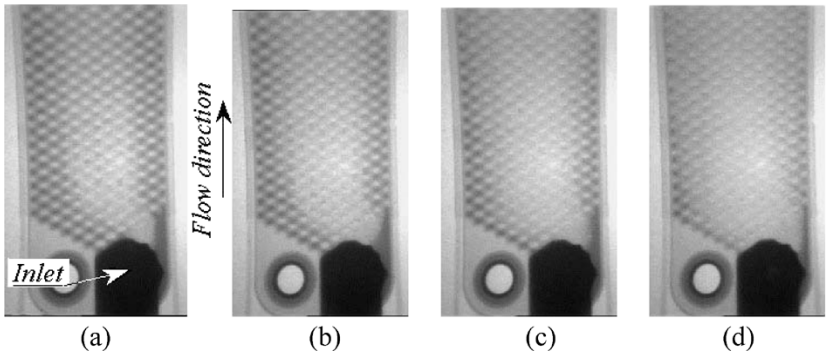

Fig. 4. Original visualized image by SIT-tube camera ($jL = 0.5$ m/s). (a) $j_G = 0.5$ m/s; (b) $j_G = 2.5$ m/s; (c) $j_G = 3.5$ m/s; and (d) $j_G = 12.0$ m/s.

In single-channel experiments, dynamic flow behaviors were visualized and void fractions were calculated. On the other hand, in multichannel experiments, cross-sectional average liquid fractions in the each channel were measured and the effect of inlet conditions was considered.

II. Experimental Apparatus and Methods

Flow visualization experiments were conducted by utilizing the JRR-3m thermal neutron radiography facility at the Japan Atomic Energy Research Institute (JAERI), Tokai, Japan. Two kinds of camera were used. A silicon intensified target (SIT) tube camera was used for dynamic behavior observations. Continuous images were recorded by a video recorder with 30 frames per second (fps) and were digitized with 256 (8 bit) intensity levels and 512×512 image elements. A cooled charged-coupled device (C-CCD) camera was used for high-resolution measurements. Still images consisting of 1000×1018 image elements were photographed with an exposure time of four seconds, and were digitized with 16 384 (14 bit) intensity levels.

A schematic diagram of the experimental apparatus is shown in Fig. 2. Water and air were used as the working fluids. Air was fed to a mixing section **7** from an air compressor through a pressure regulating valve **4** and a gas flow meter. Water in a tank **1**, was fed by a pump **2** to the mixing section **7** through a cooler **3** to maintain the temperature and a water flow meter. Two-phase flows formed in the mixing section flew into the lower part of a test section placed vertically in an irradiation room. A commercial plate heat exchanger (Hisaka Works, Ltd., type BX) made from stainless wavy plates was used as the test section. The plate configuration is shown in Fig. 3(a). Wavy shape of 6.4 mm in pitch and 1.4 mm in height is formed by the pressing process of 0.45-mm-thick sheets. The wave is inclined 30° to the horizontal plane. A net-like conduit is formed by superposition of two plates with bilateral symmetrical wavy shape. The average hydraulic diameter of the net-like conduit was 3.36 mm. Two-phase mixtures perpendicularly flew into the test section from the lower hole of 23-mm diameter. Neutron beam was irradiated at the front face perpendicularly.

A vertical cross section of the distributing header of a multichannel test section is shown in Fig. 3(b). The multichannel test section has 18 parallel channels. The hole in the each plate forms the cylindrical distributing header of 23 mm in diameter and 69.7 mm in length. Neutron beam was irradiated from the side of the test section in order to visualize the each channel individually.

III. Results and Discussion

A. Single Channel Plate Heat Exchanger

Original visualized images by SIT-tube camera are shown in Fig. 4(a)–(d) for the constant liquid volumetric flux j_L of 0.5 m/s and varied gas volumetric flux j_G of 0.5, 2.5, 3.5, and 12.0 m/s. At the j_G of 0.5 m/s [Fig. 4(a)], the area filled with liquid was

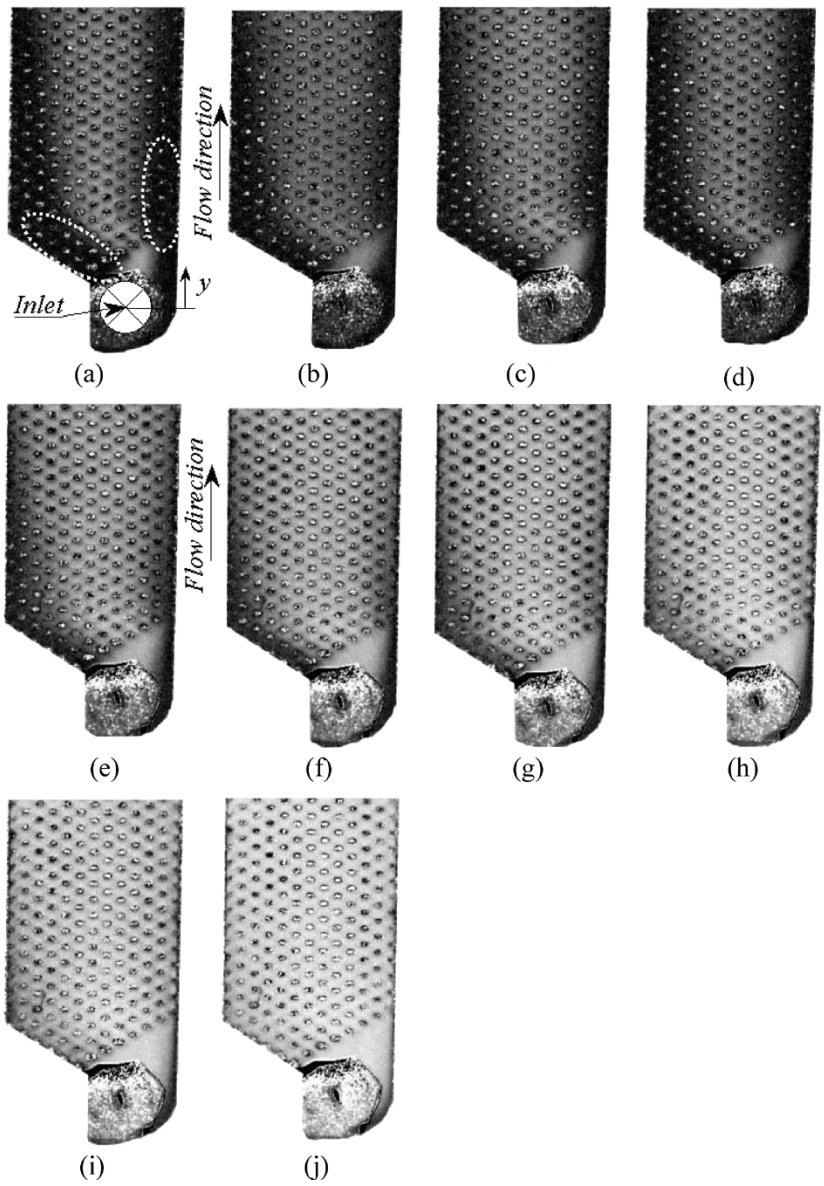

Fig. 5. Two-dimensional void fraction distribution calculated from images by C-CCD camera ($j_L = 0.5$ m/s). (a) $j_G = 0.5$ m/s; (b) $j_G = 0.8$ m/s; (c) $j_G = 1.3$ m/s; (d) $j_G = 1.7$ m/s; (e) $j_G = 3.0$ m/s; (f) $j_G = 4.9$ m/s; (g) $j_G = 7.5$ m/s; (h) $j_G = 12.3$ m/s; (i) $j_G = 19.0$ m/s; and (j) $j_G = 31.0$ m/s.

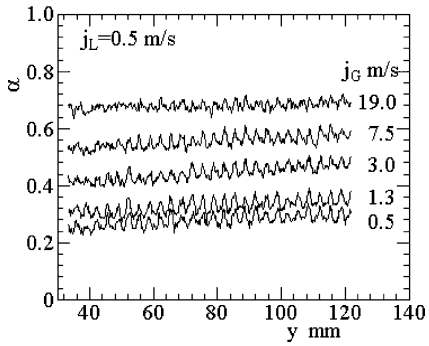

Fig. 6. Cross-sectional average void fraction.

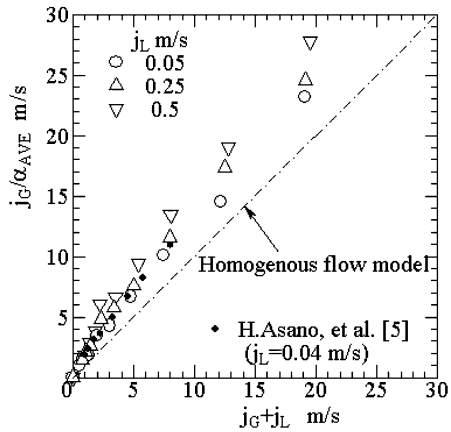

Fig. 7. Average void fraction in the net-like conduit.

observed frequently. That is to say, gas phase was flowing in the net-like condition intermittently. On the other hand, at the higher gas velocity above 3.5 m/s, gas phase was flowing continuously. Under every condition, gas phase tended to flow at the center, and the area where gas phase was flowing became larger with the increase of j_G. Liquid stagnation was observed at nodal points in the area with gas flow.

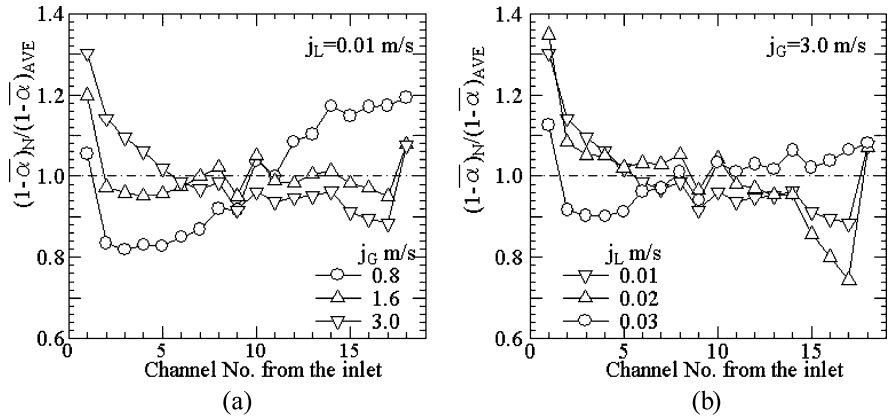

Fig. 8. Liquid distribution in a multi channel plate heat exchanger at $\mathrm{y} = 60$ mm. (a) Effect of gas flow rate. (b) Effect of liquid flow rate.

A brightness of two-phase flow image $S_{tp}(\mathrm{x},\mathrm{y})$ is expressed as

$$S_{tp}(x,y) = G(x,y)exp\left[-\rho_w\mu_{mw}t_w(x,y) - \{1-\alpha(x,y)\}\rho_L\mu_{mL}t(x,y)\right] + O_{tp}(x,y) \quad (1)$$

where subscripts of w and L mean wall and liquid, and $t(\mathrm{x},\mathrm{y})$ and $\alpha(\mathrm{x},\mathrm{y})$ mean thickness of two-phase flow area and average void fraction along the neutron beam at coordinate (x, y), respectively. $G(\mathrm{x},\mathrm{y})$ is the gain and $O_{TP}(\mathrm{x},\mathrm{y})$ is the offset. The void fraction can be calculated from gas-liquid two-phase flow image by the following equation using two kinds of images, i.e., without liquid ($\alpha = 1$, $S_1(\mathrm{x},\mathrm{y})$) and filled liquid ($\alpha = 0$, $S_0(\mathrm{x},\mathrm{y})$):

$$\alpha(x,y) = \frac{ln\left\{\frac{[S_{tp}(x,y)-O_{tp}(x,y)]}{[S_0(x,y)-O_0(x,y)]}\right\}}{ln\left\{\frac{[S_1(x,y)-O_1(x,y)]}{[S_0(x,y)-O_0(x,y)]}\right\}}. \quad (2)$$

It is necessary for quantitative measurements to estimate these offset values under the each experimental condition. In this experiment, the umbra method proposed by Kobayashi [6] was applied to measure the offset values. A cadmium tape was used as a neutron absorber, and was placed at the front of the test section. Average brightness in the umbra of the cadmium tape was used as the offset value and was measured under the each condition.

Two-dimensional void fraction distributions are shown in Fig. 5(a)–(j) in grayscale. These results were calculated from visualized images by the C-CCD camera with an exposure time of 4 s. White spot noises due to direct irradiation on CCD tips were removed by a morphological filter [7]. Nonhomogenous liquid distributions were clearly shown. That is to say, void fraction was high at the center and was very low at the both side, especially, in the area near the inlet [indicated by dotted lines in Fig. 5(a)]. However, for the j_G above 19 m/s, liquid distributions seemed to be homogenous.

Flow direction distributions of cross-sectional average void fraction, are plotted in Fig. 6 against the distance y indicated in Fig. 5(a). The void fraction periodically fluctuated in a constant range under every condition. These fluctuations might be caused by the change in cross-sectional area and liquid stagnation at nodal points in the net-like conduit. Void fraction gradually increased with the distance y, but the increase was a little.

Average void fractions in the net-like conduit were measured and are plotted in Fig. 7. The horizontal and the vertical axis show total volumetric flux and gas mean velocity, respectively. Our previous results on air-water two-phase flows in a simulated single-channel test section [5] are also plotted. Calculated results based on the homogenous model on the assumption that gas and liquid phase flow with the same velocity are plotted by a chain line. In the evaluation of pressure loss characteristics of gas-liquid two-phase flows in a vertical channel, pressure loss due to gravity is necessary in order to evaluate frictional pressure. Average void fraction is needed in calculation of pressure loss due to gravity. Though the homogenous model is sometimes used for void fraction estimation, the obtained values of j_G/α were higher than those by the homogenous model. That means lower void fraction and larger velocity difference between gas and liquid phase. On the other hand, it can be seen that our previous results agreed with these measured results quantitatively.

B. Multichannel Plate Heat Exchanger

Liquid thickness along neutron beam can be calculated from a two-phase flow image by the following equation using the image without liquid, ($\alpha = 1$, $S_1(\mathrm{x},\mathrm{y})$):

$$[1-\alpha(x,y)]\,t(x,y) = \frac{1}{\rho_L\mu_{mL}}ln\left\{\frac{S_1(x,y)-O_1(x,y)}{S_{tp}(x,y)-O_{tp}(x,y)}\right\}. \quad (3)$$

From projection images by the irradiation in the direction parallel with the plate, the sum total of liquid thickness in the each channel in a cross-section was calculated using (3). Assuming that the volume of conduit at arbitrary cross section is the same, the ratio on the sum total of liquid thickness is equivalent to the ratio on cross-sectional average liquid fraction. Calculated results at 60 mm upward from the inlet ($y = 60$ mm) are plotted in Fig. 8(a) and (b). The vertical axis shows liquid volumetric fraction normalized by the average value. In Fig. 8(a), at the lower j_G, liquid fraction became higher with the deeper channel due to the higher liquid momentum. However, at the higher j_G, the liquid distribution has the opposite tendency with the case of lower j_G. Liquid fraction became lower with the deeper channel. On the other hand, in Fig. 8(b), the same tendency was observed. That is to say, liquid distribution strongly depended on the balance gas and liquid flow rate. Under every condition, the liquid fraction at the first channel from the inlet was high. The reason might be that liquid phase easily stagnated at the enlarged section.

IV. Conclusion

As a nondestructive test of flows in plate heat exchanger, adiabatic air-water two-phase flows in a commercial one were visualized by thermal neutron radiography. The obtained results are summarized as follows.

For a single channel, gas phase tended to flow at the center of the net-like conduit and liquid fraction at the both side was higher. However, in the case of higher gas volumetric flux above 19 m/s, liquid distributions seemed to be homogenous.

For a multichannel, liquid distribution into the each channel strongly depended on the inlet conditions. In the case of higher liquid flow rate and lower gas flow rate, liquid fraction became higher with the deeper channel due to the larger liquid momentum. However, in the case of lower liquid flow rate and higher gas flow rate, the opposite tendency in liquid distribution, that is lower with the deeper channel, was observed.

References

[1] O. Charee, R. Jurkowski, A. Bailly, M. Altazin, and S. Meziani, *Compact Heat Exchangers*, G. P. Celata, B. Thonon, A. Bontemps, and S. Kandlikar, Eds. Pisa, Italy: Edizioni, 2002, pp. 207–212.

[2] Y. Shiomi, S. Nakanishi, and T. Uehara, *Compact Heat Exchangers*, G. P. Celata, B. Thonon, A. Bontemps, and S. Kandlikar, Eds. Pisa, Italy: Edizioni, 2002, pp. 393–397.

[3] C. Tribe and H. Müller-Steinhagen, "Gas-liquid flow in plate-and-frame heat exchangers–Part I: Pressure drop measurements," *Heat Transfer Eng.*, vol. 22, no. 1, pp. 5–11, Jan. 2001.

[4] ——, "Gas-liquid flow in plate-and-frame heat exchangers–Part II: Two-phase multiplier and flow pattern analysis," *Heat Transfer Eng.*, vol. 22, no. 1, pp. 12–21, Jan. 2001.

[5] H. Asano, N. Takenaka, and T. Fujii, *Compact Heat Exchangers*, G. P. Celata, B. Thonon, A. Bontemps, and S. Kandlikar, Eds. Pisa, Italy: Edizioni ETS, 2002, pp. 387–392.

[6] H. Kobayashi *et al.*, "Macroscopic cross section measurements and defect detection in materials using neutron radiography technique," *J. Nucl. Sci. Technol.*, vol. 29, no. 11, pp. 1–9, Nov. 1992.

[7] Y. Motomura, A. Ono, and K. Sonoda, "Application of morphological filters to noise suppression in neutron radiography image," in *Proc. 5th World Conf. Neutron Radiography*, Berlin, Germany, 1997, pp. 229–236.